Supplement of Biogeosciences, 22, 7745–7767, 2025
https://doi.org/10.5194/bg-22-7745-2025-supplement

Biogeosciences
Open Access

Supplement of

Wind and phytoplankton dynamics drive seasonal and short-term variability of suspended matter in a tidal basin

Gaziza Konyssova et al.

Correspondence to: Gaziza Konyssova (gaziza.konyssova@awi.de)

Supplementary Materials

Methods. Model Validation

Table S1. Performance of the model in reproducing these key tidal constituents at stations List TG, Havneby TG, and Vidaå TG. Amplitudes (A, cm) and phases (*φ*, °) were compared between the model and observations applying RMSD measure.

station	tide	simulations	observation
List TG	M2	*A*: 76.7 *φ*: 023.9	*A*: 77.9 *φ*: 023.9
	S2	*A*: 14.8 *φ*: 094.6	*A*: 12.9 *φ*: 094.6
	N2	*A*: 11.9 *φ*: 358.2	*A*:13.3 *φ*: 358.2
	O1	*A*: 7.04 *φ*: 267.7	*A*: 8.33 *φ*: 269.3
	K1	*A*: 5.79 *φ*: 063.9	*A*: 5.80 *φ*: 056.7
	Q1	*A*: 1.9 *φ*: 210.8	*A*: 2.64 *φ*: 210.8
	M4	*A*: 5.08 *φ*: 202.5	*A*: 5.08 *φ*: 214.9
		RMSD *A*: 1.79 (cm) *φ*: 5.4(°)	
Havneby TG	M2	*A*: 73.9 *φ*: 033.5	*A*: 79.8 *φ*: 024.8
	S2	*A*: 13.0 *φ*: 113.8	*A*: 19.5 *φ*: 094.9
	N2	*A*: 9.48 *φ*: 355.2	*A*: 13.4 *φ*: 359.2
	O1	*A*: 6.54 *φ*: 278.5	*A*: 8.33 *φ*: 269.3
	K1	*A*: 5.85 *φ*: 077.5	*A*: 5.80 *φ*: 056.7
	Q1	*A*: 2.62 *φ*: 211.1	*A*: 2.64 *φ*: 210.8
	M4	*A*: 7.71 *φ*: 207.5	*A*: 7.84 *φ*: 224.9
		RMSD *A*: 3.72 (cm) *φ*: 12.3(°)	
Vidaå TG	M2	*A*: 63.4 *φ*: 041.3	*A*: 63.4 *φ*: 042.4
	S2	*A*: 14.9 *φ*: 113.1	*A*: 14.9 *φ*: 113.1
	N2	*A*: 9.75 *φ*: 018.4	*A*: 9.78 *φ*: 018.3
	O1	*A*: 6.95 *φ*: 284.4	*A*: 6.95 *φ*: 284.5
	K1	*A*: 5.58 *φ*: 079.3	*A*: 5.58 *φ*: 079.4
	Q1	*A*: 1.80 *φ*: 217.7	*A*: 1.78 *φ*: 217.7
	M4	*A*: 4.77 *φ*: 014.5	*A*: 4.77 *φ*: 025.9
		RMSD *A*: 0.01 (cm) *φ*: 4.3(°)	

Methods. Neural Network

The NN was implemented in several steps using a feedforward architecture with three hidden layers, consisting of 100, 40, and 20 neurons, respectively. Each neuron acts as a simple processing unit that transforms input into output using a mathematical function. In this case, we used a hyperbolic tangent (tanh) sigmoid transfer function, which maps input values into the range between –1 and 1 and enables the model to capture complex, non-linear relationships between environmental inputs and SPM concentrations. The output layer employed a linear activation function. The Levenberg–Marquardt algorithm is used as the learning function. For training, 60% of arbitrarily chosen SPM measurements were used, while the remaining data were split for validation and testing. A separate NN was developed for each station, and the datasets for different stations were not combined.

Table S2. Input features used in the Neural Network (NN) model to predict SPM concentrations. The model was first trained on winter-only data (abiotic parameters), then extended to all seasons by incorporating biological proxy variables.

Model	Feature	Unit
Basic physical predictors (baseline model)	Wind speed at the time of sampling	m/s
	Averaged wind speed prior sampling – 13: 6h, 12h, 18h, 24h, 48h, 72h, 96h, 120h, 144h, 168h, 192h, 216h, 240h	m/s
	Dominant wind direction prior sampling – 2: 6h, 12h	degrees (°)
	Salinity	PSU
	Sea surface height (SSH)	m
	Sea surface height gradient (ΔSSH)	m
Additional biological proxies	Sea surface temperature	°C
	Light availability - weekly sum of sunshine hours prior to sampling	Hours

Results. Dominant Wind Directions

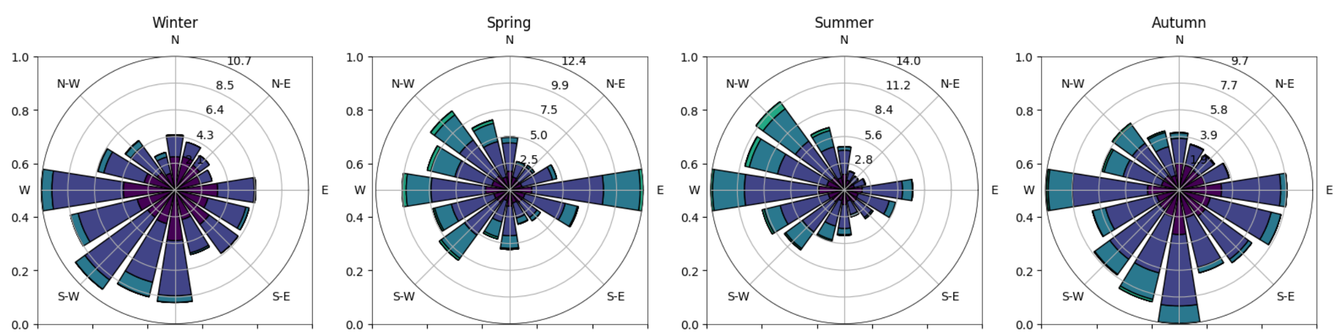

Figure S1. Dominant wind directions in seasons.

Results. Monthly Wind Memory

Figure S2: This figure presents the monthly variations in the correlation between wind speed and SPM across different wind memory intervals, ranging from short-term (1 hour) to long-term (240 hours). Each panel corresponds to a specific month, displaying Pearson correlation coefficients for both the shallow and deep stations. Orange bars represent the shallow station, while the blue bars represent the deep station.

During winter, the correlation between wind speed and SPM is generally higher than in summer (Fig. S2). At the shallow station, correlation values peak within the first 12–18 hours, then slightly decline for longer wind memory intervals. This suggests that in shallow waters, the wind conditions at the time of sampling have an immediate reflection at the SPM levels. At the deep station, correlations are generally lower but gradually increase with longer wind memory intervals (~120 hours), followed by a plateau, indicating that deep-water SPM reflects rather the average wind speed for a prolonged duration before the sampling.

In the spring and autumn months, the correlation patterns show more complex patterns. In April, for example, the correlation at the shallow station is highest at the time of sampling but decreases sharply as longer wind memory is considered. In contrast, months such as October and November exhibit a more gradual increase in correlation as wind memory extends.

During summer, particularly in June, July, and August, the correlation between wind speed and SPM is significantly weaker. As noted in Section 3.1.2, wind direction also shows no clear linear relationship with SPM, so this reduced summer correlation suggests that other mechanisms, beyond direct wind forcing, may be influencing SPM levels during this period. At the deep station, summer correlations remain low but increase slightly with longer wind averaging intervals, indicating that even in summer, accumulated wind forcing over multiple days can have a delayed effect on deep-water SPM.

Results. Influence of SSH

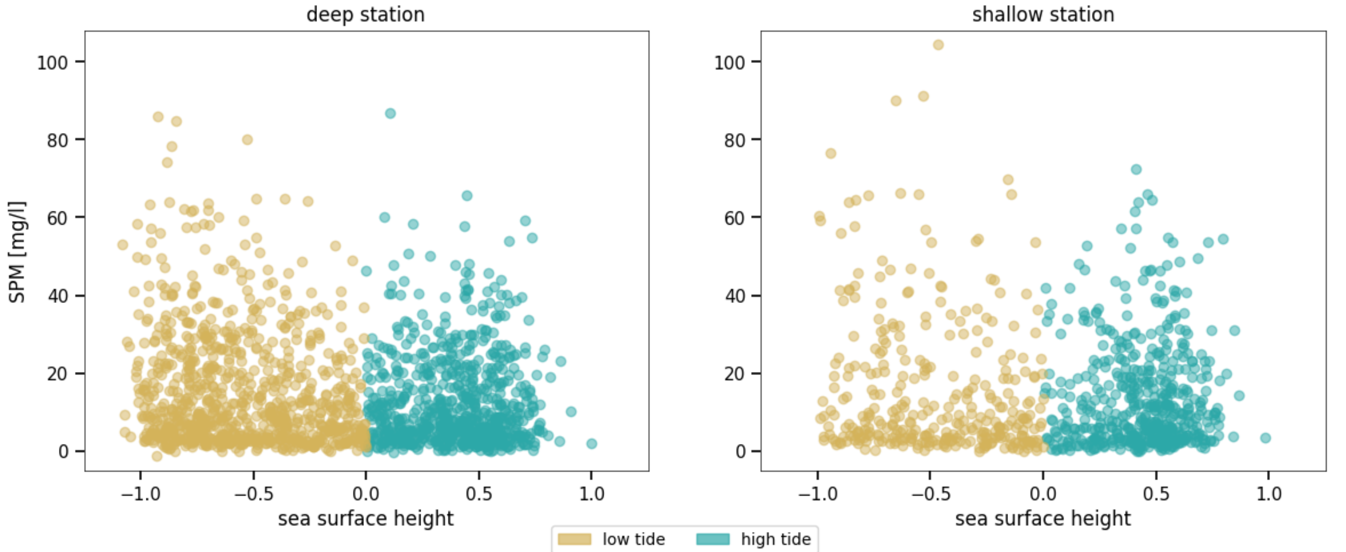

Figure S3: SPM concentrations VS sea surface height (SSH), where SSH<0 is low tide and SSH>0 is high tide.

SPM concentrations tend to be higher during low tide (SSH < 0) and lower during high tide (SSH > 0), as shown in Fig. S3. This relationship reflects the effect of tidal water level on sampling depth. At low tide, when the water column is shallower, the samples capture more of the resuspended particulate matter, whereas at high tide, SPM concentrations are slightly smaller with the increased water depth. This effect produces a more pronounced gradient at the shallow station, where the total water depth is around 2 meters. Here, tidal fluctuations significantly alter the vertical position of the sample relative to the seabed, making SPM concentrations more sensitive to SSH changes. In contrast, at the deeper station (~10 meters depth), this vertical shift has a smaller relative impact on the sampling position, and therefore on SPM values.

Beyond modulating sampling depth, tidal forcing itself also promotes resuspension. Due to the presence of tidal asymmetry in the area, characterized by a difference in maximum and mean velocities between flood and ebb phases, the resulting resuspension is also not entirely balanced across the tidal cycle. To capture this phase-dependent variability, the gradient of sea surface height is included as an input feature in the neural network model.

The phase of the tidal cycle determines the velocity field. Due to the strong role of non-linear processes in the domain, ebb and flood are not equally strong in terms of maximum and mean velocities. This asymmetry is evident in Fig. S4, where SPM concentrations are showntogether with the SSH gradient (derivative is calculated using forward scheme, time step is ~5 min).

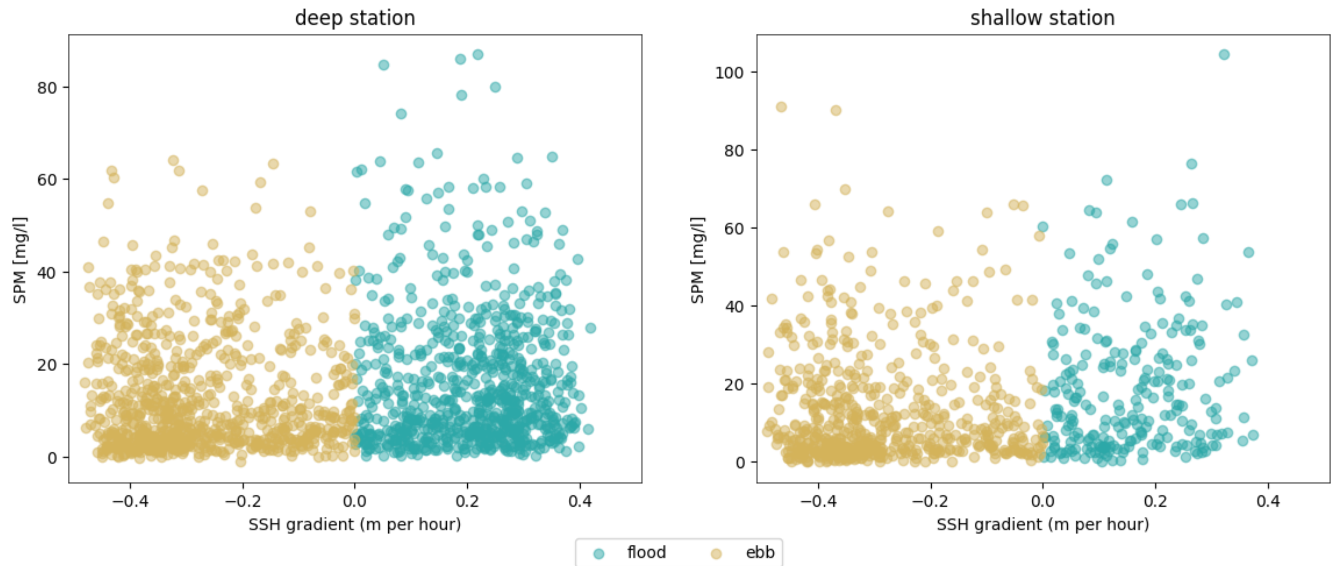

Figure S4: Relationship between suspended particulate matter (SPM) concentrations and tidal phase, represented by the gradient of reconstructed sea surface height (SSH), at the deep and shallow stations (left, middle). Ebb and flood phases show asymmetric distributions, with highest SPM concentrations occurring during flood.

Results. Neural Network

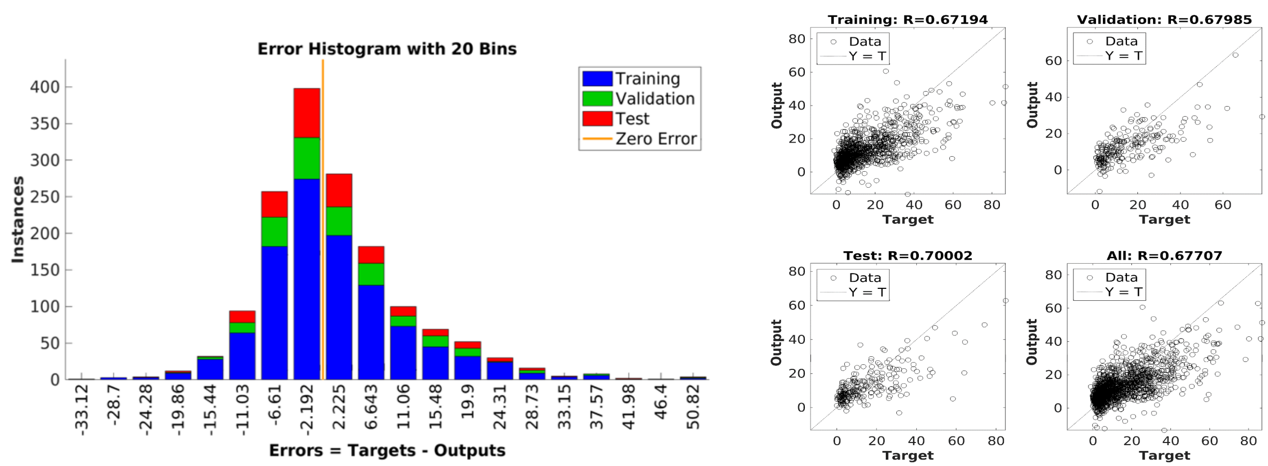

Figure S5. Performance of the neural network (NN) trained on the data from all seasons for the deep station. Left: Error histogram showing the distribution of prediction errors (in mg/L) for training, validation, and test subsets. Right: Regression plots comparing predicted vs. observed SPM values, with correlation coefficients (R) for each data subset. Due to the overall qualitative similarity between the pictures for deep and shallow stations, only the deep station is presented here. Errors are in mg/L.

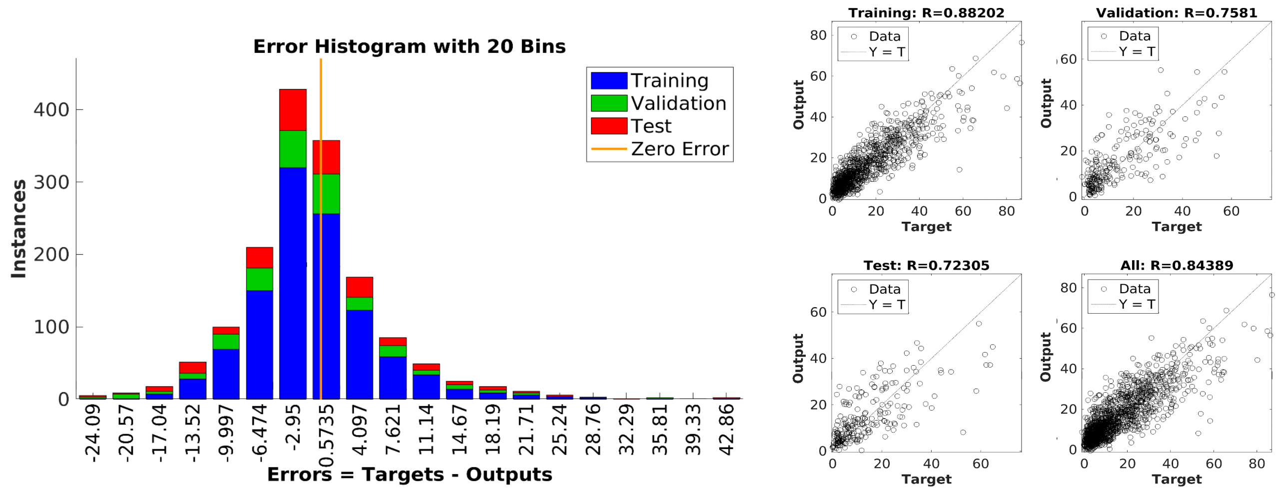

Figure S6. Performance of the neural network (NN) trained on full dataset with the abiotic + two additional (biological) features for the deep station. Left: Error histogram showing the distribution of prediction errors (in mg/L) for training, validation, and test subsets. Right: Regression plots comparing predicted vs. observed SPM values, with correlation coefficients (R) for each data subset. Due to the overall qualitative similarity between the pictures for deep and shallow stations, only the deep station is presented here. Errors are in mg/L.

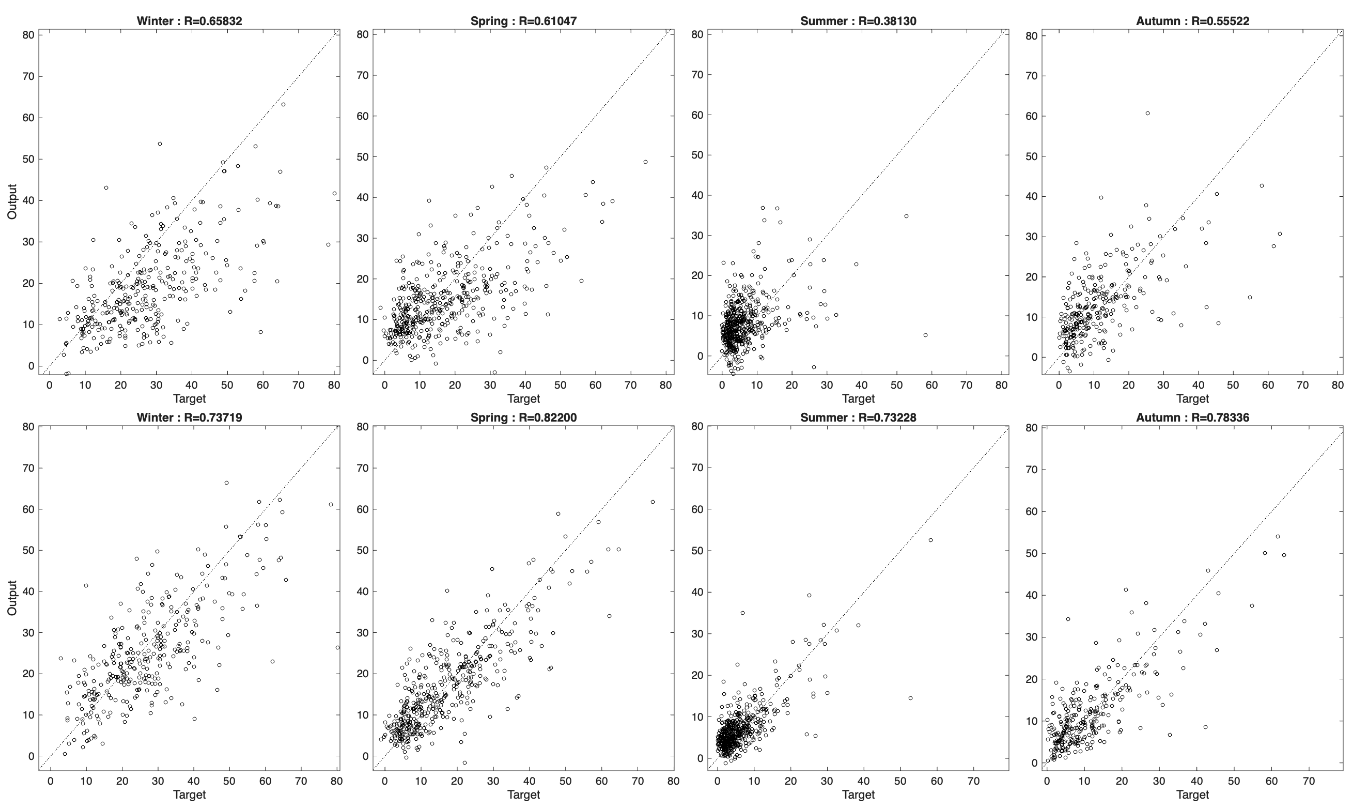

Figure S7. Regression analysis of neural network (NN) performance for seasonal subsets. Upper row: results for an NN trained on all-season abiotic input features and applied to spring, summer, and autumn data. Lower row: results for an NN trained on all-season abiotic input features supplemented *with biological proxies* (temperature and sunshine duration) and applied to the same seasonal subsets.

Table S3. Seasonal observed and predicted SPM concentrations at the shallow and deep stations, based on neural network models trained with abiotic features only and with additional biological proxies (temperature and light). Values are shown as mean and median [mg L⁻¹]. Regression coefficients (R) are provided for each season.

Shallow station:

seasons		observed	NN: all seasons abiotic	NN: all seasons abiotic + temperature, light
winter	mean, [mg/L]	28.5	20.0	23.2
	median, [mg/L]	24.4	17.5	22.5
			R = 0.72	*R = 0.82*
spring	mean, [mg/L]	15.6	10.8	15.9
	median, [mg/L]	11.3	8.75	12.3
			R = 0.65	*R = 0.84*
summer	mean, [mg/L]	6.8	5.0	8.2
	median, [mg/L]	3.9	3.3	6.0
			R = 0.6	*R = 0.71*
autumn	mean, [mg/L]	12.8	10.4	14.5
	median, [mg/L]	7.5	7.9	11.6
			R = 0.65	*R = 0.85*

Deep station:

seasons		observed	NN: all seasons abiotic	NN: all seasons abiotic + temperature, light
winter	mean, [mg/L]	27.6	19.2	25.6
	median, [mg/L]	25.9	17.2	23.6
			R = 0.66	*R = 0.73*
spring	mean, [mg/L]	16.5	14.8	16.6
	median, [mg/L]	13.3	13.17	14.3
			R = 0.61	*R =0.82*
summer	mean, [mg/L]	6.2	7.9	7.1
	median, [mg/L]	4.2	7.1	5.8
			R =0.38	*R =0.73*
autumn	mean, [mg/L]	11.6	12.6	11.9
	median, [mg/L]	8.5	10.8	9.3
			R = 0.56	*R =0.78*